Available online at www.sciencedirect.com

ScienceDirect

www.elsevier.com/locate/jes

JES JOURNAL OF ENVIRONMENTAL SCIENCES

www.jesc.ac.cn

Fog composition along the Yangtze River basin: Detecting emission sources of pollutants in fog water

Xianmang Xu[1], *Jianmin Chen*[1,2,*], *Chao Zhu*[1], *Jiarong Li*[1], *Xiao Sui*[1], *Lu Liu*[1], *Jianfeng Sun*[2]

1. *School of Environmental Science and Engineering, Environment Research Institute, Shandong University, Jinan 250100, China*
2. *Shanghai Key Laboratory of Atmospheric Particle Pollution and Prevention (LAP), Institute of Atmospheric Sciences, Fudan University, Shanghai 200433, China*

ARTICLE INFO

Article history:
Received 6 May 2017
Revised 15 September 2017
Accepted 18 September 2017
Available online 12 October 2017

Keywords:
Fog water chemistry
Three-stage CASCC
Trace metal elements

ABSTRACT

To investigate the fog chemistry along the Yangtze River basin, a field observation experiment was performed from Shanghai to Wuhan during November 2015. Fifteen fog water samples were collected by using a three-stage Caltech Active Strand Cloud water Collector (CASCC). The three-stage CASCC was mounted on the board of a ship. PH, electrical conductivity (EC), H_2O_2, HCHO, S(IV), ten inorganic ions, seven organicacids and sixteen trace metal elements were measured in this study. The pH of fog water samples ranged from weakly acidic (pH 4.3) to weakly alkaline (pH 7.05) and the EC ranged from 32.4 to 436.3 μS/cm. The main cations in fog water were NH_4^+ and Ca^{2+}, accounting for 12.35% and 29.07% of those inorganic ions, respectively. In addition, SO_4^{2-} and NO_3^- contributed to 25.52% and 12.93% to total anion concentrations respectively. Moreover, the dominant kinds of organicacids were formate and oxalate, occupying 45.28% and 28.03% of the total organicacids, respectively. For trace metal elements in fog samples, Al, Fe, Zn, and Ba revealed 34.6%, 16.4%, 19.3%, and 20.9% contributions to these sixteen trace element concentrations, respectively. The results indicated that pollutants were mainly from human activities, including fossil fuel combustion, biomass burning, steel-making, stone quarrying and sand digging. Besides, natural sources including natural background levels and long-range transport of sea salt particles also aggravated the pollution levels in the fog events along the Yangtze River.

Introduction

Fog is a ubiquitous atmospheric phenomenon which often occurs in low temperature and high relative humidity atmosphere. Similar as cloud, fog has an important effect on the transformation of aerosol particles and trace gases (Biswas et al., 2008). Fog is generally formed near surface. It usually has higher pollutant concentrations than cloud (Pengfei et al., 2011). Also, fog as a special state of aerosols can promote atmospheric particles and soluble gases transfer into liquid phase (Ming and Russell, 2004; Collett et al., 2008; Gilardoni et al., 2014). The transfer of the soluble species promotes wet deposition and the modifications of the physical and chemical properties of aerosol particles (Kaul et al., 2011). The chemical components of fog droplets could be changed during the heterogeneous chemical processes (Ervens et al., 2011). Thus, the chemical reactions in fog droplets play an important role on the formation of secondary aerosols (Li et al., 2013). Although scholars had focused on the fog chemistry for several years due to its high pollutant concentrations, previous studies of fog and cloud chemistry usually focused on mountains, coasts or cities, while fewer studies focused on the Yangtze River basin.

* *Corresponding author. E-mail:* jmchen@sdu.edu.cn (Jianmin Chen).

https://doi.org/10.1016/j.jes.2017.09.018
1001-0742/

The length of the Yangtze River is more than 6300 km. This study was carried out along the middle and lower reaches of the Yangtze River. The total observed river way length is about 1000 km from Shanghai to Wuhan. The sailing path went through many heavy-populated cities including Shanghai, Nanjing and Wuhan *etc*. The urban development and industrial activity can contribute to a rising aerosol concentration (Chune et al., 2008). When air is stagnated in densely populated or industrial areas, the pollution concentrations usually keep at high levels (Raja et al., 2009). Since Shanghai is one of the densely populated cites in China, several fog samples were collected and measured in Shanghai from March 2009 to March 2010. The result showed that the main inorganic ions in the fog water were SO_4^{2-}, NO_3^-, NH_4^+ and Ca^{2+} in Shanghai (Pengfei et al., 2011). SO_4^{2-}, NH_4^+ and Ca^{2+} were the dominant ions in the fog collected in Nanjing during December 2006 and December 2007 (Chunsong et al., 2010). Most of the pollution species in the fog of Nanjing were expected to come from industrial emissions, traffic pollution, construction dusts and biomass burning.

The fog pollutions occurred at the densely populated cities located along the Yangtze River has been concerned in previous study. These observation experiments were helpful to understand the air pollution conditions in those cities. However, most of these sampling sites were stationary in previous studies. This paper shows a mobile observation of fog chemistry from Shanghai to Wuhan. In this study, a three-stage CASCC was mounted on the board of a moving ship. Fog samples were collected during ship sailing. The sampling sites were five areas rather than five stationary sites. Therefore these fog samples were more representative for the chemical properties of fog water along the Yangtze River basin. Ten inorganic ions, seven organicacids and sixteen trace metal elements in fog samples and other parameters concerned with fog water chemistry were analyzed in this study.

1. Experiment and methods

1.1. Ship trajectory and sampling sites

The ship set out from Shanghai Waigaoqiao wharf (31°21′31″N, 121°36′40″E) to Wuhan (30°37′04″N, 114°19′59″E) from November 21 to 29, 2015. The total sailing distance is about 1000 km (Fig. 1). Ship trajectory went through five provinces and municipalities located at the middle and lower reaches of the Yangtze River, including Shanghai, Jiangsu, Anhui, Jiangxi and Hubei. The fog samples were collected during fog events when the visibility was less than 1 km. The sampling areas were mainly distributed in Jiangsu, Anhui and Hubei provinces (Fig. 1). The first three sampling areas were in Jiangsu province. The first and second sampling areas were close to Nantong and Zhenjiang ports, respectively. Also, these two sampling areas were the closest sites to the coast (less than 100 km). The third sampling area was near to the populous city of Nanjing. The fourth sampling area was located at Ma'anshan which was one of the top ten steeling bases in China. The last sampling area was in Hubei province and near to the city of Wuhan.

1.2. Weather conditions

Weather condition is one of the key factors for fog samples collection. Fog situation directly affects the collection volume of fog samples. The cloud and fog covers, water vapor and aerosol optical depth are important parts of the weather condition (Kourtidis et al., 2015). In order to describe the weather conditions in sampling areas, the satellite images of Yangtze River basin from November 22 to 29, 2015 were captured from the Earth Observing System Data and Information System (EOSDIS) which was a part of NASA's Earth Science Data Systems Program. As shown in Fig. 2, white represented cloud and fog; green and blue expressed water; gray and brown indicated land. There were only two sunny days in the middle and lower reaches of the Yangtze River basin from November 22 to 29, 2015. Heavy foggy day occurred on November 24 and two samplings were carried out. In addition, sampling was performed once on November 22, 23 and 29, respectively.

1.3. Fog collection

Fog water samples were collected using the three-stage CASCC; an updated version of the size fractions CASCC designed for the collection of cloud droplets in two size fractions was provided (Demoz et al., 1996). The structure and working principle of this instrument were described in great detail by Spiegel et al. (2012). There was a fan located at the rear of the collector to draw air

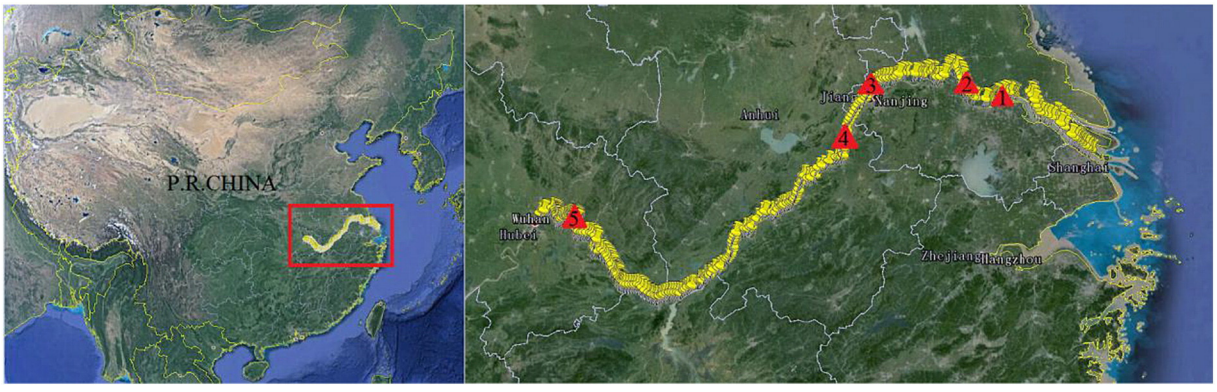

Fig. 1 – Ship trajectory and sampling sites (from Shanghai to Wuhan). ▲ sampling sites which are the location at the approximate middle time of sampling process. Ship trajectory were drawn by the GPS coordinates.

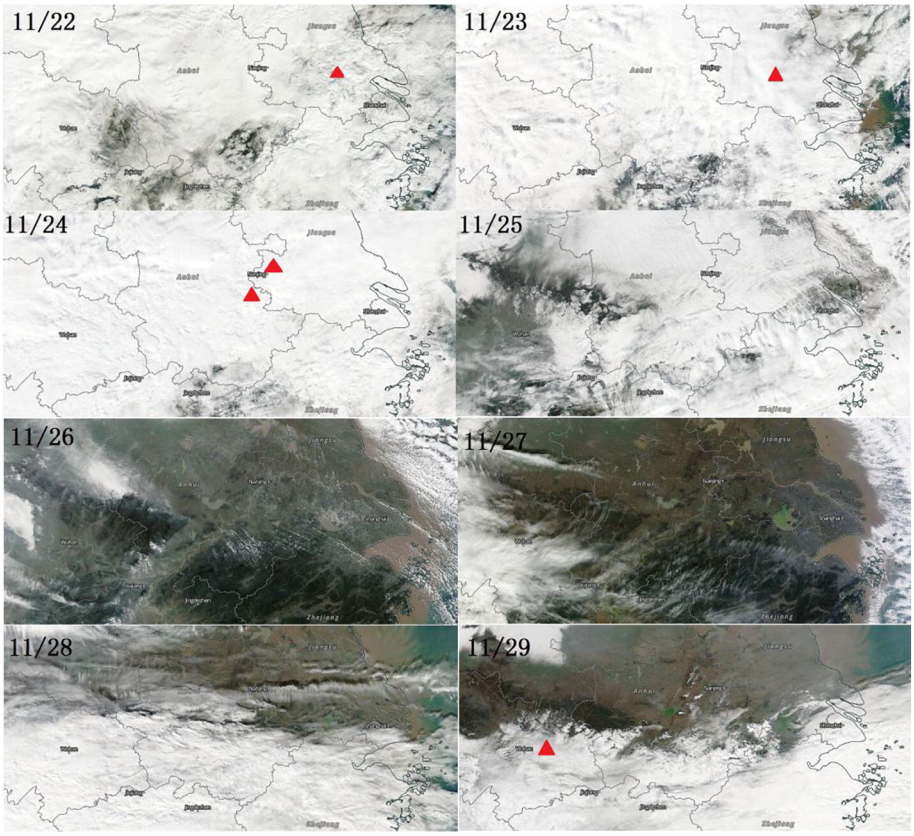

Fig. 2 – Satellite images and sampling sites. ▲ sampling sites. Satellite images form EOSDIS worldview (https://earthdata.nasa.gov/labs/worldview/).

through a duct. A number of inclined Teflon rods of three different sizes were inlaid in the duct as impaction obstacles. When air passes through the duct, fog droplets were impacted on the Teflon collection strands and coalesced into fog water due to gravity and aerodynamic drag. The clotted fog water flowed down the Teflon rods into a Teflon sample trough and went through a Teflon tube into polyethylene collection bottles. The rods of the largest diameter were inlaid at the front of the collector (Spiegel et al., 2012).

The three-stage CASCC was operated with a volume flow of 19 m^3/min. The fog droplet sizes were collected with about 50% efficiency and cut for three stages, with an approximately 22, 16, and 4 μm diameter, respectively (Spiegel et al., 2012). In fact, the fog droplet sizes could not be perfectly separated into three particle diameter stages. When fog droplets were collected using three-stage CASCC, it had a little overlap in sizes on adjacent stages. Therefore, in terms of droplet sizes, the differences in the measured compositions of fog samples were conservative estimates of the actual differences in compositions. Besides the droplets drawn by the fan, it was possible that some droplets were blown into the CASCC by the ambient wind. The largest size of droplets collected in the first stage could be estimated up to about 100 μm under the conditions of ambient wind (Spiegel et al., 2012). In order to inhibit the raindrops blown by the wind, a downward facing was deployed in the front of the collector when rain was expected. Due to the exhaust located at the stern of the ship, the fog collector was mounted on the prow of ship to avoid the emission impact from the ship itself. The collector was placed approximately 1.5 m above the deck of ship. The total height of collector was more than 3 m above the surface of river. Prior to sampling, the three-stage CASCC was cleaned by ultrapurewater (>18.2 MΩ·cm).

On the basis of the fog conditions, sampling times were 6 to 9 hr for per fog sample. After sampling, parts of the fog samples were detached from polyethylene collection bottles to be measured including pH, EC, H_2O_2, HCHO and S(IV) immediately. Parts of the residues were filled into number of small polyethylene bottles and frozen at −20°C in freezer for chemical composition analysis. The rest parts of fog samples for trace metal element measurement were pretreated with 10% (in volume) HCl to acidified fog samples and inhibit the chelation reaction, then filled into glass bottles and refrigerated under near-freezing temperatures. And 10% (in volume) concentrated nitricacid were added to samples to dissolve the trace metals before measurement. During the campaign, five sets of three-stage fog samples were collected. However, the volume of the second stage in the third sampling was too little to analyze the whole chemical components.

1.4. *Chemical analysis*

To prevent the impact of ambient factors and volatile, pH, EC, H_2O_2, HCHO and S(IV) were measured on-site. The pH and EC

were measured by a portable pH and conductivity compound instrument (Model Jenco-6350, Jenco Electronics, Ltd., USA). The instrument had been calibrated before measuring. The concentrations of H_2O_2 were measured by 4-hydroxyphenylacetic acid fluorescencemethod using a fluorospectrophotometer (Model F96Pro, Shanghai Lengguang Technology Co., Ltd., China). The concentrations of HCHO were measured by pentanedione spectrophotometric method using an ultraviolet-visible spectrophotometer (Model L5, Shanghai Lengguang Technology Co., Ltd., China). The S(IV) concentrations were determined with formaldehyde absorbing-pararosaniline spectrophotometry method using the same UV spectrophotometer with HCHO measurement. The methods for the H_2O_2 as well as HCHO and S(IV) measurements were referred to Guo et al. (2012). During measuring, ultrapure water was used as blanks to ensure the reliability of data. Furthermore, ten inorganic ions (Na^+, NH_4^+, K^+, Mg^{2+}, Ca^{2+}, F^-, Cl^-, NO_2^-, SO_4^{2-}, NO_3^-) and seven organicacids (formate, acetate, propionate, butyrate, mesylate, oxalate, lactate) were analyzed by ion chromatography (Dionex, ICS-90). In order to eliminate the interference of large particles to the ionicanalysis, fog samples were filtered through a targeted specifically 0.2 μm nylon filter before entering into the equipment. Besides the familiar analysis to fog water as shown above, the concentrations of sixteen heavy metal elements (Al, V, Cr, Mn, Fe, Co, Ni, Cu, Zn, As, Se, Sr, Cd, Ba, Tl, Pb) in the fog samples were also measured by atomic absorption spectrometry.

2. Results and discussion

2.1. Basic information and concentrations of H_2O_2, HCHO, and S(IV)

The investigated campaign of the Yangtze River was carried out in November 2015. Fog occurs frequently in the Yangtze River basin during this season. Low temperature and high relative humidity are conducive to the formation of radiation fog (Wrzesinsky and Klemm, 2000). There were seven fog days in the middle and lower reaches of the Yangtze River basin from November 21 to 29, 2015. In total, fifteen fog samples were collected during this campaign. The basic information of fog samples are shown in Table 1. The pH value of the three-stage fog samples ranged from weakly acidic (pH 4.3) to weakly alkaline (pH 7.05). As shown in Table 1, the pH value of every stage in the same fog process was very similar, although the fog samples were collected with different droplet sizes. In other words, the sizes of fog droplets are not a determinant factor on the pH value. The pH of fog is only subjected to the balance between acidic and basic inputs (Pengfei et al., 2011). Similar with pH, the electric conductivity is a fundamental characteristic that reflected the total ionic content in fog water. As shown in Table 1, the EC ranged from 32.4 to 436.3 μS/cm in this campaign. Compared with the pH value, the EC showed a diversity among the different droplet sizes.

In addition to the pH and EC, the concentrations of H_2O_2, HCHO and S(IV) were taken measurement on-site. H_2O_2 was considered as one of the most important oxidant in the chemical process of fog water (Harris et al., 2013). HCHO was a hazardous pollutant to human body (Facchini et al., 1990). The S (IV) as the precursor of SO_4^{2-} was widely concerned in the study of fog or cloud water (Zhang and Tie, 2011; Harris et al., 2013). Therefore, it is significative to pay attention to the concentrations of H_2O_2, HCHO and S(IV) in fog water. Table 1 shows the results of H_2O_2, HCHO and S(IV) in fog samples. The concentration distributions of these three species were diverse in different droplet sizes, but had no obvious regularities. It might be related to the unstable characteristics and the source emissions of these three species (Collett et al., 1998). However, it's worth mentioning that the concentrations of these three species in the fourth sampling were significantly lower than those in the third sampling. From the view of the sampling time and satellite images (Fig. 2), the fog samples collected at the third and fourth sampling were in the same fog event that had a long time fog process. H_2O_2 as the oxidant for S(IV) was consumed early in the fog or cloud lifetime. The S(IV) was oxidized to sulfate and added to the CCN. This result is consistent with numerous

Table 1 – Description of basic information during fog collection and concentrations of H_2O_2, HCHO & S(IV).

Date	Time	Three-stage CASCC	Volume (ml)	pH	EC (μS/cm)	H_2O_2 (μM)	HCHO (μM)	S(IV) (μM)
Nov. 22–23	20: 50–03: 00	I (>22 μm)	10	5.44	233.1	7.3	8.9	11.3
		II (17–22 μm)	8	5.45	265.2	11.4	14.7	14.0
		III (4–16 μm)	15	5.42	325.7	14.4	10.8	11.4
Nov. 23	09: 00–15: 00	I (>22 μm)	17	5.40	241.0	8.8	24.8	15.9
		II (17–22 μm)	8	5.15	127.5	10.7	19.2	12.3
		III (4–16 μm)	13	5.46	436.3	12.4	18.3	12.5
Nov. 24	01: 00–08: 00	I (>22 μm)	15	6.38	49.9	10.0	31.7	42.9
		II (17–22 μm)	5	6.06	39.7	12.8	42.3	44.4
		III (4–16 μm)	125	6.02	42.4	8.1	25.1	21.2
Nov. 24	10: 00–16: 30	I (>22 μm)	70	4.46	59.5	4.5	11.7	8.6
		II (17–22 μm)	25	4.30	32.4	4.2	10.6	3.1
		III (4–16 μm)	175	4.86	38.5	4.1	11.7	8.8
Nov. 28–29	23: 00–08: 00	I (>22 μm)	60	7.05	81.5	3.7	18.2	23.7
		II (17–22 μm)	10	7.03	37.1	18.8	33.9	115.5
		III (4–16 μm)	45	6.96	39.4	4.8	23.1	27.0

CASCC: Caltech Active Strand Cloud water Collector; EC: electrical conductivity.

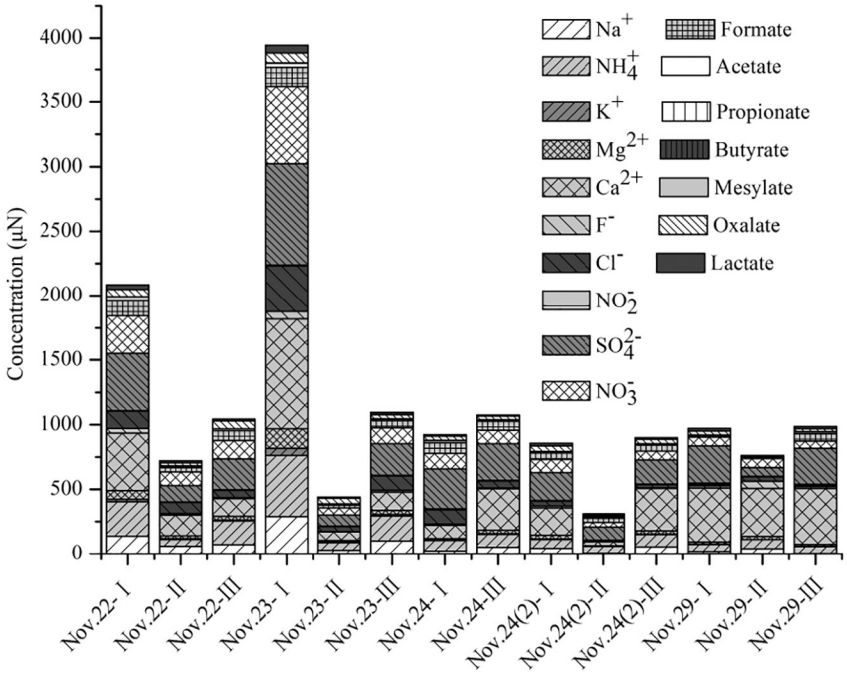

Fig. 3 – Ions concentrations (μN) of every fog water sample.

previous studies (Pandis and Seinfeld, 1990; Erel et al., 1993; Harris et al., 2013).

2.2. Chemical compositions of fog water

Inorganic ions and organicacids are the most important components of fog chemistry. The concentrations of main ionic compositions in fog samples are shown in Fig. 3. The fog sample of the second stage in the third sampling on November 24 is not included due to the lack of fog water for analysis. Because of the influence of geographical location and surrounding environment, the pollutant concentrations in fog samples collected at the first and second sampling sites were significantly higher than those at other sites. The pollutant emissions from transportation near Nantong and Zhenjiang ports could be one of the important factors for the high pollutions at the first two sites. The emissions from factories and industries along both sides of the Yangtze River also could not be ignored. There was an obvious distribution characteristic of ion concentrations depend on droplet sizes in the first two

Table 2 – Distribution of ion concentrations in large and small droplets.

Species	I-stage large droplet concentration [μN]		III-stage small droplet concentration [μN]		Large/small droplet fraction ratio		
	Minimum	Maximum	Minimum	Maximum	Minimum	Maximum	Mean
Na^+	18.2	288.3	4.8	100.2	0.43	3.80	1.97
NH_4^+	54.4	475.4	51.9	194.8	0.73	2.44	1.29
K^+	3.3	52.0	1.4	10.2	0.73	5.12	2.48
Mg^{2+}	12.7	152.0	14.3	32.6	0.46	4.66	1.91
Ca^{2+}	102.7	849.1	136.2	435.0	0.32	5.99	2.24
F^-	10.3	59.2	4.0	15.3	1.10	4.70	3.10
Cl^-	12.6	356.6	7.5	111.2	1.45	3.21	2.12
NO_2^-	3.3	7.4	3.0	9.3	0.80	1.83	1.32
SO_4^{2-}	216.9	784.4	186.5	283.9	1.05	3.20	1.67
NO_3^-	66.1	594.8	56.8	143.4	1.14	4.83	2.12
Formate	8.3	148.2	44.2	76.4	0.15	2.61	1.33
Acetate	6.3	32.8	9.9	15.8	0.40	3.29	1.76
Propionate	1.2	2.0	1.2	1.6	0.82	1.49	1.15
Butyrate	0.3	0.4	0.3	0.4	0.97	1.07	1.02
Mesylate	0.2	0.3	-	-	-[a]	-[a]	-[a]
Oxalate	29.9	75.2	21.7	60.1	0.94	2.33	1.42
Lactate	13.9	62.0	8.8	20.0	1.17	3.10	2.05

- Sample concentrations less than the detection limit observed.
-[a] Where concentrations less than the detection limit occur, the large/small drop fraction ratio can't be calculated.

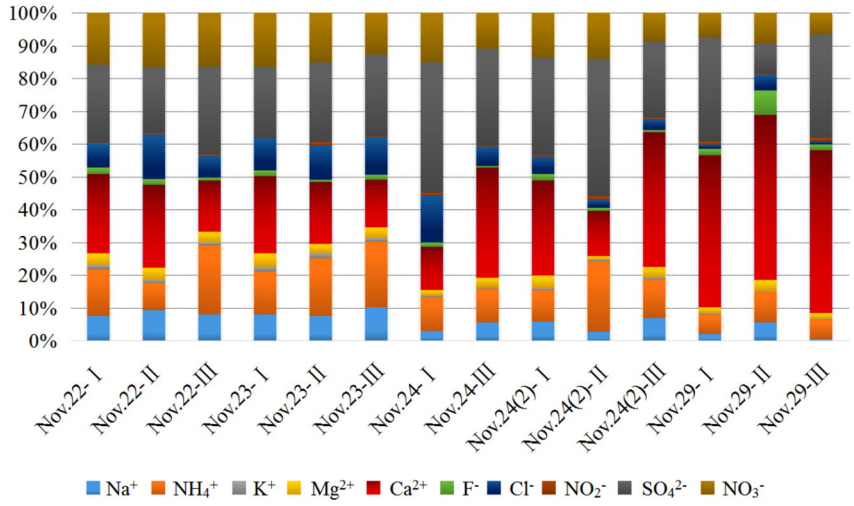

Fig. 4 – Inorganic ion concentrations percentage of every fog water sample.

sampling sites. The main ions were concentrated in the fog samples of the first stage. The fraction ratios of concentrations between large and small fog droplets are shown in Table 2 for expounding the distribution characteristics of ion concentrations in large and small droplets.

The fraction ratio of ionic concentrations between large and small fog droplets is one of the main parameters for studying the ion distributions depend on droplet sizes (Moore et al., 2004). Due to the physical and chemical processes in fog droplets are very complex and the ion distributions cannot be observed directly, the fraction ratios of ion concentrations between large and small fog droplets have important implications for expounding the ion distributions depend on droplet sizes in fog water. Table 2 shows the concentration distributions of inorganic ions and organicacids in large and small droplets. The minimum values of large/small droplets fraction ratios of F^-, Cl^-, SO_4^{2-} NO_3^- and lactate are larger than 1. It means that those ions are mainly concentrated in large droplets in the five sampling areas.

2.3. Proportions of inorganic ions and organicacids

The normality proportions of inorganic ions and organicacids in fog samples provide the bases for the research of the chemical compositions and ion distributions in fog water (Moore et al., 2004). As shown in the Fig. 4, the main cations in the fog water collected along the Yangtze River were NH_4^+ and Ca^{2+}, while the dominated anions were SO_4^{2-} and NO_3^-. Due to the influence by sea salt, the proportions of Na^+ decreased with the increased distance to coastline. NO_3^- presented the same tendency with Na^+, which possibly attributed to the decrease of anthropogenic emissions with the increased distance to coastline. The proportions of Ca^{2+}

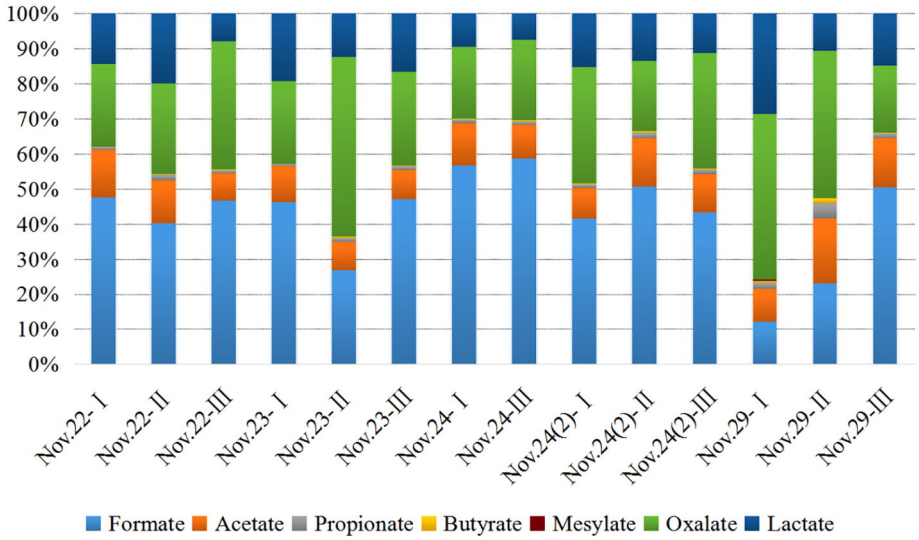

Fig. 5 – Organicacid concentrations percentage of every fog water sample.

in the last sampling sites were higher than those in other sites, which might be due to the quarrying operations and sand excavations along the Yangtze River. Organicacids similar with inorganic ions are the important components in fog water. Fig. 5 shows the proportions of organicacids in fog samples. Formate and oxalate were dominant in the fog samples while acetate and lactate were also non-negligible.

2.4. Source analysis of pollution emission

The average concentrations can be regarded as the comprehensive evaluations of the pollutions in the sampling areas. Table 3 summarizes the average pH values, EC (μS/cm) and volume-weighted mean concentrations of inorganic ions, H_2O_2, HCHO, S(IV) and their comparisons with other studies. The ratio of the sum cation (Na^+, NH_4^+, K^+, Mg^{2+}, Ca^{2+}) to the sum anion (F^-, Cl^-, NO_2^-, SO_4^{2-}, NO_3^-) was 1.11, which could be attributed to the presences of HCO_3^- and CO_3^{2-} that were not measured. This phenomenon is similar to the result in Nanjing (Chunsong et al., 2010). The average concentrations of species in fog samples were calculated separately according to the sampling sites. From the view of geography, the concentrations of main species in fog water showed significant differences related to sampling sites. The concentrations of these species decreased gradually from coastal to inland along the Yangtze River. On the one hand, this variation was affected by the natural factors including geographical position and sea wind. On the other hand, human factors also could not be ignored including the anthropogenic emissions from stationary and mobile sources. The lower reaches of the Yangtze River is one of the most economically developed regions in China, which has a large number of populations, factories and industries. The pollutants from human activities played an important role in fog water chemistry process. Thus the main anthropogenic species, NH_4^+, SO_4^{2-} and NO_3^- in the first and second sampling sites were significantly higher than that in other three inland sampling sites. Most of the ions presented the same trend with NH_4^+ SO_4^{2-} and NO_3^- along the Yangtze River, excepted for Ca^{2+}, F^- and NO_2^-.

As shown in Table 3, the concentration tendencies of Mg^{2+} was highly consistent with Na^+. Mg^{2+} might be similar to Na^+ was mainly from the droplet scavenging of sea salt and soil dust particles (Pengfei et al., 2011). The NH_4^+ probably originated from human activities that include industrial and traffic emissions, biomass burning, human and animal excretions, and vegetative emissions in farmland (Chunsong et al., 2010; Boris et al., 2016). In this study, the industrial emissions were mainly from nitrogenous fertilizer plants and chemical reagent factories on both sides of the Yangtze River. The traffic emissions were mainly from the waterway transport ships, the vehicles at ports and the vehicles on the road near the river. As one of the primary elements in the plant straw, potassium could be released to atmosphere in the case of biomass burning. Therefore, K^+ mainly comes from biomass burning besides from sea salt and soil dust particles (Pengfei et al., 2011). Frequent construction activities were considered as the primary sources of Ca^{2+}, involving house building, road reconstruction and infrastructure maintaining (Millet et al., 1996). Moreover, the dust from the quarrying operations on both sides of the Yangtze River was another important source of Ca^{2+} in fog water. F^- was

Table 3 – Average pH value, EC (μS/cm) and volume-weighted mean concentrations of inorganic ions, H_2O_2, HCHO & S(IV) and comparison with other studies.

Fog event	pH	EC	Na^+	NH_4^+	K^+	Mg^{2+}	Ca^{2+}	F^-	Cl^-	NO_2^-	SO_4^{2-}	NO_3^-	H_2O_2	HCHO	S(IV)	Year	Reference
		(μS/cm)	(μN)	(μN)	(μN)	(μN)	(μN)	(μN)	(μN)	(μN)	(μN)	(μN)	(μM)	(μM)	(μM)		
Nov. 22–23	5.44	274.7	88.5	177.4	22.1	39.1	235.7 (232)[a]	17.2	87.3	3.8	272.5 (262)[a]	179.1	11.5	11.2	12.0	2015	This work
Nov. 23	5.34	268.3	168.8	292.5	27.0	81.2	442.5 (435)[a]	31.7	223.2	4.6	453.0 (433)[a]	319.6	10.4	21.4	14.0		
Nov. 24	6.15	44.0	47.4	94.1	5.2	24.8	287.0 (285)[a]	4.5	60.0	4.1	276.7 (271)[a]	101.5	8.4	26.3	24.2		
Nov. 24(2)	4.54	43.5	46.8	84.6	21.2	23.7	269.8 (268)[a]	7.1	27.6	3.1	186.6 (181)[a]	73.9	4.2	11.6	8.2		
Nov. 28–29	7.01	52.7	14.9	54.8	2.4	16.3	421.0 (420)[a]	21.9	13.6	7.7	265.0 (263)[a]	62.7	5.4	21.5	33.0		
San Joaquin Valley, USA	6.49	–	5.8	1008.1	12.0	3.5	8.9	–	14.6	–	117.5	483.0	4.1	46.4	5.5	1995	Collett et al. (1998)
Po-valley, Italy	6.9	–	40	730	20	20	10	–	70	20	50	450	–	–	–	2010	Giulianelli et al. (2014)
Mt. Whiteface, USA	3.88	79.6	3.7	149.3	2.1	7.4	26.6	–	7.2	0.87	220.4	79.2	–	–	–	2006	Aleksic et al. (2009)
Mt. Niesen, Switzerland	6.4	34.4	43.0	143.5	5.0	12.6	46.8	1.6	10.6	1.1	72.3	87.0	–	–	–	2006–2007	Michna et al. (2015)
Shanghai, China	5.97	2050	809	4005	224	318	2064	–	1178	–	2830	2416	–	–	–	2009–2010	Pengfei et al. (2011)
Nanjing, China	5.9	681	1282	6654	383	347	3772	493	1010	282	6969	945	–	–	–	2006–2007	Chunsong et al. (2010)

– No data given; EC: electrical conductivity.

[a] $[nssCa^{2+}]$ and $[nssSO_4^{2-}]$ were obtained through $[nssCa^{2+}] = [Ca^{2+}] - 0.12\ [Na^+]$ and $[nssSO_4^{2-}] = [SO_4^{2-}] - 0.044\ [Na^+]$, respectively (Degefie et al., 2015).

mainly from soil dust and the combustion of fossil fuel. Besides transporting with sea salt and soil dust particles, the concentration of Cl^- was probably attributed to the industries along the Yangtze River, because an important source for Cl^- was believed to be associated with coal burning (Chunsong et al., 2010). The concentrations of NO_2^-, SO_4^{2-} and NO_3^- were mainly influenced by industrial and traffic emissions. Ships in the Yangtze River and the industries on the both sides of the river were the main sources of NO_2^-, SO_4^{2-} and NO_3^-. In addition to all above emission sources, long-range transport of fine particles was also an important factor influencing the chemical compositions of fog water (Fig. 6).

Back trajectories were determined using the HYSPLIT trajectory model. The starting height was set at 50 m, which was more similar to the altitude of sampling sites. Each trajectory was initiated at the approximate middle time of every sampling process. The selection of a 24 hr period for the back trajectories was on account of the mobile sampling instrument. As shown in Fig. 6, the influence of marine aerosols should not be neglected in this campaign except for the last sampling. The sea salt carried by wind would increase the concentrations of pollutants in fog water.

2.5. *Trace metal elements*

Previous research showed that the transition metal elements of Fe and Mn played an important role in the catalyzed oxidation of the S(IV) in cloud (Harris et al., 2013). The heavy metal elements of Pb, Cd and Zn are harmful to human health (Viard et al., 2004). The concentration of heavy metal element is also an important parameter of environment pollution (Lin et al., 2016; Chen et al., 2016). In this study, sixteen trace metal elements (Al, V, Cr, Mn, Fe, Co, Ni, Cu, Zn, As, Se, Sr, Cd, Ba, Tl, Pb) in the fog samples were measured in this study. The concentrations of the sixteen trace elements in fifteen fog samples were shown in Table 4. Al, Fe, Zn and Ba dominated the detected elements in fog water, accounting for 34.6%, 16.4%, 19.3% and 20.9% of the sixteen elements, respectively. The natural background levels should be contributed to the high concentrations of the four elements. At the same time, human activities were also an important factor leading to high concentrations of the elements in fog water. The highest concentrations of Al and Zn appeared at the second sampling site, which might be related to the emissions from the ports and industries. The highest concentration of Fe appeared at the fourth sampling site, which was likely attributed to the steel industry at Ma'anshan. The highest concentration of Ba appeared at the last sampling site, which was probably concerned with quarrying operations and sand excavation. Besides the above four elements, Mn and Cu also occupied little proportions of these elements, accounting for 3.5% and 1.3%, respectively. Among those elements, Fe and Mn could enhance the catalysis oxidation process of S(IV) in fog or cloud water (Harris et al., 2013).

The enrichment factors (EFs) for individual trace elements were used to infer their general crust, sea salt or anthropogenic source. The EF values were calculated using the following Eqs. (1) and (2):

$$EF_{crust}X = (X/Al)_{fog}/(X/Al)_{crust} \quad (1)$$

$$EF_{seawater}X = (X/Al)_{fog}/(X/Al)_{seawater} \quad (2)$$

where $EF_{crust}X$ and $EF_{seawater}X$ were the enrichment factors of element X; $(X/Al)_{crust}$ values were calculated on the basis of the background contents of elements in Chinese soils (Wei et al.,

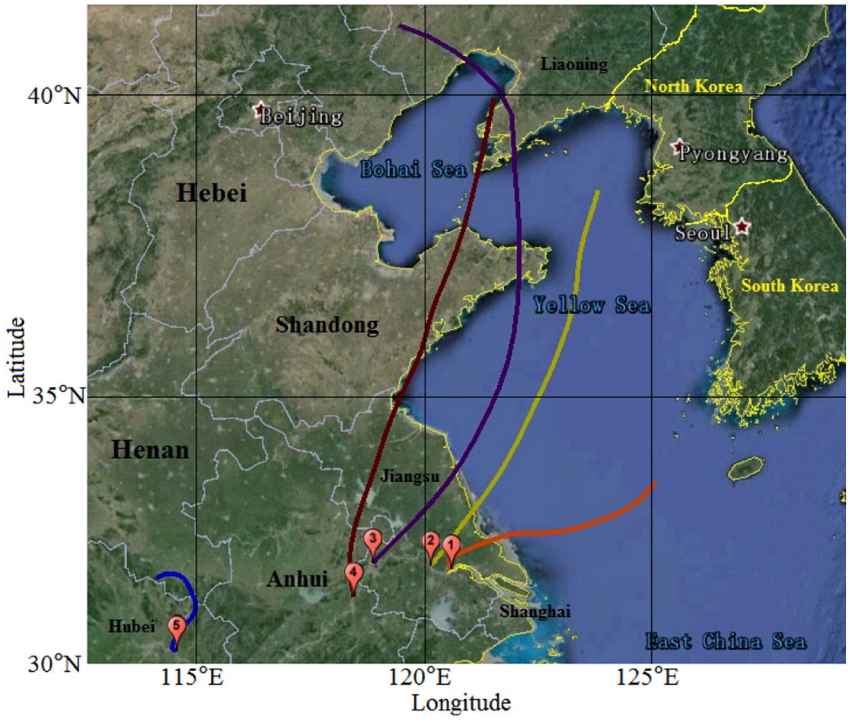

Fig. 6 – Back trajectories of air masses intercepted at five sampling sites during fog events (24 hr at 1 hr time resolution).

Table 4 – Metal elements concentrations of every fog water sample (unit: μg/L).

Sampling time	Three-stage CASCC	Al	V	Cr	Mn	Fe	Co	Ni	Cu	Zn	As	Se	Sr	Cd	Ba	Tl	Pb
Nov. 22–23, 2015 20:50–03:00	I (>22 μm)	241.7	2.2	5.6	15.4	132.2	0.1	2.6	5.0	37.0	1.8	1.0	5.0	0.2	180.7	–	0.7
	II (17–22 μm)	228.0	2.3	5.3	13.6	139.0	0.1	2.7	2.4	32.6	1.9	0.9	4.1	0.2	183.2	–	1.1
	III (4–16 μm)	607.8	4.8	4.1	73.0	177.0	1.3	11.7	50.8	478.5	2.7	1.9	32.0	1.8	250.9	0.1	13.7
Nov. 23, 2015 09:00–15:00	I (>22 μm)	640.9	7.0	6.2	108.5	238.3	1.6	12.0	34.9	887.7	5.5	5.8	48.2	4.1	254.3	0.2	7.1
	II (17–22 μm)	592.3	5.8	4.0	70.5	232.0	1.0	8.8	40.0	547.4	4.9	4.4	27.9	2.8	264.4	0.2	14.9
	III (4–16 μm)	467.0	5.2	7.2	52.8	234.4	0.6	6.3	13.4	403.6	4.9	4.6	19.0	2.7	266.0	0.1	6.5
Nov. 24, 2015 01:00–08:00	I (>22 μm)	294.0	1.8	3.6	15.5	142.0	0.1	1.5	1.7	26.0	1.9	0.6	6.9	0.2	232.9	–	2.3
	II (17–22 μm)	277.5	2.2	5.9	14.0	160.0	0.2	2.5	2.5	27.0	2.2	1.1	5.3	0.2	221.3	–	1.5
	III (4–16 μm)	312.6	5.1	4.0	36.6	158.9	0.5	4.3	11.1	245.7	3.6	1.7	25.2	1.7	216.6	0.1	4.5
Nov. 24, 2015 10:00–16:30	I (>22 μm)	485.1	3.9	4.7	45.3	218.6	0.5	4.3	13.6	180.1	3.5	2.1	16.8	1.1	253.1	0.2	9.8
	II (17–22 μm)	386.0	2.9	4.3	27.1	251.0	0.3	3.2	12.1	108.4	3.2	2.1	8.8	0.8	255.0	0.1	11.3
	III (4–16 μm)	366.9	3.6	4.1	29.8	237.5	0.3	2.9	8.3	142.7	3.0	2.2	9.1	1.0	200.7	0.2	10.5
Nov. 28–29, 2015 23:00–08:00	I (>22 μm)	340.2	3.0	5.5	38.4	146.4	0.3	2.3	6.6	69.8	4.7	1.3	27.3	1.8	269.7	0.1	1.0
	II (17–22 μm)	342.2	1.9	3.9	23.4	162.5	0.2	2.3	4.8	35.9	2.2	0.7	10.5	0.7	265.5	–	1.5
	III (4–16 μm)	281.0	3.0	6.0	35.7	145.8	0.3	2.5	4.8	37.7	4.7	1.1	27.0	1.3	231.6	0.1	1.1

– Below the detection limit; CASCC: Caltech Active Strand Cloud water Collector.

1991); $(X/Al)_{seawater}$ values were adopted from the Yangtze estuary and Pearl river delta background contents of elements (Koshikawa et al., 2007; Ouyang et al., 2006). The background values of trace metals in soil came from Wei. Most of the background contents in water came from Koshikawa. The Se and Tl values in water came from Ouyang. EFs were classified into three groups with the following standard: EFs < 10 was suggested to be crust or seasalt sources without enrichment; 10 < EFs < 100 was classified as moderate enrichment (crust or seasalt and anthropogenic sources); and EFs > 100 was considered as extreme enrichment (air pollution mainly comes from anthropogenic sources) (Li et al., 2015). Fig. 7 describes the EF values of trace elements in five sampling sites along the Yangtze River. From the $EF_{crust}X$ values, the trace elements of Zn, Se and Cd were found to be highly enriched, indicating that these elements might came from anthropogenic pollutants. According to the $EF_{seawater}X$ values, the elements with EFs > 100, including Zn and Ba, were considered as extreme enrichment, indicating that the pollution mainly came from anthropogenic sources. Besides, several trace elements, including Mn, Ni, Cu, As and Sr, were likely from mixed origins because the majority of their EFs values fell within 10–100. It is worth noting that the trace elements at the second sampling site were more obviously affected by human activity.

In addition to the EFs of trace elements, the correlation analysis of these elements was also calculated to expound the sources of pollution. As the results shown in Table 5, Zn, Se and Cd showed high positive correlations with each other, combined with the EF values, these elements were probably from the similar anthropogenic pollution sources including industrial and shipping emissions (Espinosa et al., 2004; Voutsa and Samara, 2002). Other elements like Al, Mn, Co, Ni and Cu showed high positive correlations with each other, which suggested that these elements were probably related to the dust particles in air besides from anthropogenic origin (Fang et al., 2005; Zheng et al., 2004). In addition, this result was similar to the result of EF values. It is worth mentioning that the element of Ba has a high concentration but no obvious correlation with other elements, which may indicate that the concentration of Ba in fog water has been elevated as a result of anthropogenic inputs. The enrichment has been verified by the $EF_{seawater}X$ values. In addition, many trace metal element

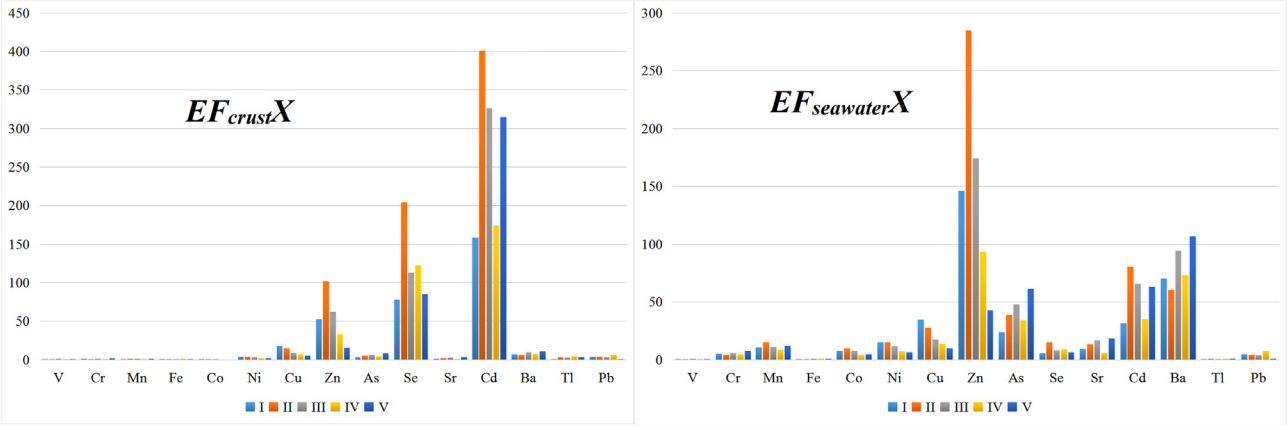

Fig. 7 – Enrichment factors (EFs) values of trace elements in five sampling sites along the Yangtze River based on the background contents of elements in crust and seawater.

Table 5 – Correlation analysis of metal elements concentrations.

	Al	V	Cr	Mn	Fe	Co	Ni	Cu	Zn	As	Se	Sr	Cd	Ba	Tl	Pb
Al	1															
V	0.83**	1														
Cr	−0.03	0.17	1													
Mn	0.92**	0.91**	0.17	1												
Fe	0.69**	0.62*	0.02	0.55*	1											
Co	0.92**	0.90**	0.07	0.98**	0.50	1										
Ni	0.91**	0.86**	0.09	0.93**	0.48	0.98**	1									
Cu	0.91**	0.77**	−0.14	0.85**	0.46	0.92**	0.95**	1								
Zn	0.90**	0.94**	0.17	0.96**	0.59*	0.96**	0.95**	0.84**	1							
As	0.58*	0.76**	0.41	0.73**	0.50	0.60*	0.50	0.42	0.64**	1						
Se	0.80**	0.89**	0.36	0.84**	0.77**	0.78**	0.76**	0.63*	0.90**	0.75**	1					
Sr	0.73**	0.83**	0.19	0.91**	0.29	0.87**	0.78**	0.71**	0.81**	0.81**	0.65**	1				
Cd	0.82**	0.94**	0.29	0.94**	0.57*	0.88**	0.81**	0.70**	0.92**	0.87**	0.90**	0.90**	1			
Ba	0.63*	0.39	−0.01	0.53*	0.44	0.45	0.38	0.42	0.41	0.58*	0.44	0.52*	0.55*	1		
Tl	0.74**	0.80**	0.17	0.78**	0.81**	0.67**	0.58*	0.52*	0.72**	0.83**	0.81**	0.70**	0.82**	0.50	1	
Pb	0.78**	0.61*	−0.36	0.57*	0.78**	0.61*	0.64**	0.77**	0.58*	0.31	0.56*	0.33	0.46	0.37	0.62*	1

* Significant at 0.05 level.
** Significant at 0.01 level.

concentrations (including Cr, As, Se, Pb *etc.*) in fog water could also be influenced by the emissions of fossil fuel combustions, industrial and waste incinerations (Li et al., 2015; Cheng et al., 2011).

3. Conclusions

An observation campaign was performed along the Yangtze River from Shanghai to Wuhan. Chemical components of the fog along the middle and lower reaches of the Yangtze River were studied. The pH values of the three-stage fog water samples collected on a moving ship ranged from weakly acidic (pH 4.3) to weakly alkaline (pH 7.05). The electrical conductivity (EC) ranged from 32.4 to 436.3 μS/cm in this campaign. The concentrations of inorganic ions in Yangtze valley were similar as in other valleys and mountains but lower than those in cities. Strong influences by sea salt and anthropic factors were observed on the fog chemical components along the Yangtze River. An obvious variation was observed with the distance to coastline, especially the concentrations of Na^+, NH_4^+, Cl^- and NO_3^-. The main cations in the fog water collected along the Yangtze River were NH_4^+ and Ca^{2+}, the main anions were SO_4^{2-} and NO_3^-, and the dominant organicacids were formate and oxalate. The ions of F^-, Cl^-, SO_4^{2-} NO_3^- and lactate were mainly concentrated in large droplets in the five fog events. In addition, sixteen trace metal elements in fifteen fog samples were also analyzed. Al, Fe, Zn and Ba dominated the detected elements in the fog samples, accounting for 34.6%, 16.4%, 19.3% and 20.9% of the sixteen trace elements, respectively. Due to the influence of various factors including anthropogenic and natural emissions, the concentrations of the trace elements appeared regional difference along the Yangtze River.

Acknowledgments

This work was supported by the National Natural Science Foundation of China (Nos. 41605113, 41375126), the Taishan Scholar Grand (No. ts20120552).

REFERENCES

Aleksic, N., Roy, K., Sistla, G., Dukett, J., Houck, N., Casson, P., 2009. Analysis of cloud and precipitation chemistry at Whiteface Mountain, NY. Atmos. Environ. 43, 2709–2716.

Biswas, K.F., Ghauri, B.M., Husain, L., 2008. Gaseous and aerosol pollutants during fog and clear episodes in South Asian urban atmosphere. Atmos. Environ. 42, 7775–7785.

Boris, A.J., Lee, T., Park, T., Choi, J., Seo, S.J., Collett Jr., J.L., 2016. Fog composition at Baengnyeong Island in the eastern Yellow Sea: detecting markers of aqueous atmospheric oxidations. Atmos. Chem. Phys. 16, 437–453.

Chen, B., Stein, A.F., Castell, N., Gonzalez-Castanedo, Y., Sanchez de la Campa, A.M., Rosa, J.D., 2016. Modeling and evaluation of urban pollution events of atmospheric heavy metals from a large Cu-smelter. Sci. Total Environ. 539, 17–25.

Cheng, M., You, C., Lin, F., 2011. Sources of Cu, Zn, Cd and Pb in rainwater at a subtropical islet offshore northern Taiwan. Atmos. Environ. 45, 1919–1928.

Chune, S., Matthias, R., Hao, Z., Zihua, L., 2008. Impacts of urbanization on long-term fog variation in Anhui Province, China. Atmos. Environ. 42, 8484–8492.

Chunsong, L., Shengjie, N., Lili, T., Jingjing, L., Lijuan, Z., Bin, Z., 2010. Chemical composition of fog water in Nanjing area of China and its related fog microphysics. Atmos. Res. 97, 47–69.

Collett Jr., J.L., Katherine, J.H., Sherman, D.E., Bator, A., Richards, L. W., 1998. Spatial and temporal variations in San Joaquin Valley fog chemistry. Atmos. Environ. 33, 129–140.

Collett Jr., J.L., Herckes, P., Youngster, S., Lee, T., 2008. Processing of atmospheric organic matter by California radiation fogs. Atmos. Res. 87, 232–241.

Degefie, D.T., El-Madany, T.S., Held, M., Hejkal, J., Hammer, E., Dupont, J.C., et al., 2015. Fog chemical composition and its

feedback to fog water fluxes, water vapor fluxes, and microphysical evolution of two events near Paris. Atmos. Res. 164-165, 328–338.
Demoz, B., Collett Jr., J.L., Daube Jr., B., 1996. On the Caltech active strand cloudwater collectors. Atmos. Res. 41, 47–62.
Erel, Y., Pehkonen, S.O., Hoffmann, M.R., 1993. Redox chemistry of iron in fog and stratus clouds. J. Geophys. Res. 98, 18423–18434.
Ervens, B., Turpin, B.J., Weber, R.J., 2011. Secondary organic aerosol formation in cloud droplets and aqueous particles (aqSOA): a review of laboratory, field and model studies. Atmos. Chem. Phys. 11, 11069–11102.
Espinosa, A.J.F., Rodriguez, M.T., Alvarez, F.F., 2004. Source characterisation of fine urban particles by multivariate analysis of trace metals speciation. Atmos. Environ. 38, 873–886.
Facchini, M.C., Lind, J., Orsi, G., Fuzzi, S., 1990. Chemistry of carbonyl compounds in Po Valley fog water. Sci. Total Environ. 91, 79–86.
Fang, G.C., Wu, Y.S., Huang, S.H., Rau, J.Y., 2005. Review of atmospheric metallic elements in Asia during 2000–2004. Atmos. Environ. 39, 3003–3013.
Gilardoni, S., Massoli, P., Giulianelli, L., Rinaldi, M., Paglione, M., Pollini, F., et al., 2014. Fog scavenging of organic and inorganic aerosol in the Po Valley. Atmos. Chem. Phys. 14, 6967–6981.
Giulianelli, L., Gilardoni, S., Tarozzi, L., Rinaldi, M., Decesari, S., Carbone, C., et al., 2014. Fog occurrence and chemical composition in the Po valley over the last twenty years. Atmos. Environ. 9, 394–401.
Guo, J., Wang, Y., Shen, X., Wang, Z., Lee, T., Wang, X., et al., 2012. Characterization of cloud water chemistry at mount tai, China: seasonal variation, anthropogenic impact, and cloud processing. Atmos. Environ. 60, 467–476.
Harris, E., Sinha, B., van Pinxteren, D., Tilgner, A., Fomba, K.W., Schneider, J., et al., 2013. Enhanced role of transition metal ion catalysis during in-cloud oxidation of SO_2. Science 340, 727–730.
Kaul, D.S., Gupta, T., Tripathi, S.N., Tare, V., Collett, J.L., 2011. Secondary organic aerosol: a comparison between foggy and nonfoggy days. Environ. Sci. Technol. 45, 7307–7313.
Koshikawa, M.K., Takamatsu, T., Takada, J., Zhu, M., Xu, B., Chen, Z., et al., 2007. Distributions of dissolved and particulate elements in the Yangtze estuary in 1997–2002: background data before the closure of the three gorges dam. Estuar. Coast. Shelf Sci. 71, 26–36.
Kourtidis, K., Stathopoulos, S., Georgoulias, A.K., Alexandri, G., Rapsomanikis, S., 2015. A study of the impact of synoptic weather conditions and water vapor on aerosol-cloud relationships over major urban clusters of China. Atmos. Chem. Phys. 15, 10955–10964.
Li, Y.J., Lee, B.Y.L., Yu, J.Z., Ng, N.L., Chan, C.K., 2013. Evaluating the degree of oxygenation of organic aerosol during foggy and hazy days in Hong Kong using high-resolution time-offlight aerosol mass spectrometry (HR-ToF-AMS). Atmos. Chem. Phys. 13, 8739–8753.
Li, T., Wang, Y., Li, W.J., Chen, J.M., Wang, T., Wang, W.X., 2015. Concentrations and solubility of trace elements in fine particles at a mountain site, southern China: regional sources and cloud processing. Atmos. Chem. Phys. 15, 8987–9002.
Lin, H., Sun, T., Xue, S., Jiang, X., 2016. Heavy metal spatial variation, bioaccumulation, and risk assessment of *Zostera japonica* habitat in the Yellow River Estuary, China. Sci. Total Environ. 541, 435–443.
Michna, P., Werner, R.A., Eugster, W., 2015. Does fog chemistry in Switzerland change with altitude? Atmos. Res. 151, 31–44.
Millet, M., Sanusi, A., Wortham, H., 1996. Chemical composition of fogwater in an urban area: Strasbourg (France). Environ. Pollut. 94, 345–354.
Ming, Y., Russell, L.M., 2004. Organic aerosol effects on fog droplet spectra. J. Geophys. Res. 109, D10206.
Moore, K.F., Sherman, D.E., Reilly, J.E., Collett Jr., J.L., 2004. Drop size-dependent chemical composition in clouds and fogs. Part I. Observations. Atmos. Environ. 38, 1389–1402.
Ouyang, T.P., Zhu, Z.Y., Kuang, Y.Q., Huang, N.S., Tan, J.J., Guo, G. Z., et al., 2006. Dissolved trace elements in river water: spatial distribution and the influencing factor, a study for the Pearl River Delta Economic Zone, China. Environ. Geol. 49 (5), 733–742.
Pandis, S.N., Seinfeld, J.H., 1990. On the interaction between equilibration processes and wet or dry deposition. Atmos. Environ. 24, 2313–2327.
Pengfei, L., Xiang, L., Chenyu, Y., Xinjun, W., Jianmin, C., Collett Jr., J.L., 2011. Fog water chemistry in Shanghai. Atmos. Environ. 34, 1921–1957.
Raja, S., Raghunathan, R., Kommalapati, R.R., Shen, X., Collett Jr., J. L., Valsaraj, K.T., 2009. Organic composition of fogwater in the Texas-Louisiana Gulf Coast corridor. Atmos. Environ. 43, 4214–4222.
Spiegel, J.K., Aemisegger, F., Scholl, M., Wienhold, F.G., Collett Jr., J. L., Lee, T., et al., 2012. Stable water isotopologue ratios in fog and cloud droplets of liquid clouds are not size-dependent. Atmos. Chem. Phys. 12, 9855–9863.
Viard, B., Pihan, F., Promeyrat, S., Pihan, J.C., 2004. Integrated assessment of heavy metal (Pb, Zn, Cd) highway pollution: bioaccumulation in soil, Graminaceae and land snails. Chemosphere 55, 1349–1359.
Voutsa, D., Samara, C., 2002. Labile and bioaccessible fractions of heavy metals in the airborne particulate matter from urban and industrial areas. Atmos. Environ. 36, 3583–3590.
Wei, F., Chen, J., Wu, Y., Zheng, C., 1991. Study of the background contents of 61 elements of soils in China. Environ. Sci. 12 (04), 12–19 (in Chinese).
Wrzesinsky, T., Klemm, O., 2000. Summertime fog chemistry at a mountainous site in central Europe. Atmos. Environ. 34, 1487–1496.
Zhang, Q., Tie, X., 2011. High solubility of SO_2: evidence in an intensive fog event measured in the NCP region, China. Atmos. Chem. Phys. Discuss. 11, 2931–2947.
Zheng, J., Tan, M.G., Shibata, Y., Tanaka, A., Li, Y., Zhang, G.L., et al., 2004. Characteristics of lead isotope ratios and elemental concentrations in PM_{10} fraction of airborne particulate matter in Shanghai after the phase-out of leaded gasoline. Atmos. Environ. 38, 1191–1200.